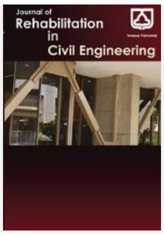

Journal of Rehabilitation in Civil Engineering

Journal homepage: https://civiljournal.semnan.ac.ir/

Effect of Steel Fiber Ratios in Thin Concrete Plate Modeling

Omer M. M. Mahdi [1,*]; Alper Buyukkaragoz [2]; Ahmet S. Unal [3]

1. Ph.D. Candidate, Department of Civil Engineering, Graduate School of Natural and Applied Sciences, Gazi University, Ankara, Turkey
2. Professor, Department of Civil Engineering, Faculty of Technology, Gazi University, Ankara, Turkey
3. Undergraduate Student, Department of Civil Engineering, Faculty of Technology, Gazi University, Ankara, Turkey
* Corresponding author: *omohanad.mahdi@gazi.edu.tr*

ARTICLE INFO

Article history:
Received: 02 July 2024
Revised: 13 August 2024
Accepted: 02 November 2024

Keywords:
Steel fiber;
Concrete retrofitting;
Compressive strength;
Tensile strength;
Flexural strength test.

ABSTRACT

Steel fiber reinforcement has emerged as a pivotal innovation in enhancing the mechanical properties of concrete, particularly in applications requiring improved tensile strength, energy absorption, and ductility, thereby making it a vital consideration in the retrofitting of reinforced concrete elements. Compression strength, splitting tensile strength, and flexural strength tests were conducted to determine the mechanical properties in term of compressive and tensile strength of concrete panels containing different proportions of steel fibers for use in the Retrofitting (thin concrete plate) of reinforced concrete elements. Steel fibers were incorporated into the concrete at volume fractions of 0%, 1%, and 2%. To compare and verify the tensile strengths obtained from the experiments, formulas provided in TS 500 and results from ANSYS 15 finite element program were utilized. In regard to the flexural strength test results, the incorporation of steel fibers in the cement mortars led to a significant increase in tensile strength, with enhancements of up to 112.5% and 137.5% for steel fiber volume fractions of 1% and 2%, respectively. Furthermore, increasing the steel fiber volume fraction to 1% and 2% notably improved the energy absorption capacity by 80 and 110 times, respectively, and the ductility ratio by 15 and 18 times, respectively.

E-ISSN: 2345-4423

How to cite this article:
Mahdı, O., Buyukkaragoz, A., & Unal, A. (2025). Effect of Steel Fiber Ratios in Thin Concrete Plate Modeling. Journal of Rehabilitation in Civil Engineering, 13(2), 147-164. https://doi.org/10.22075/jrce.2024.34414.2114

1. Introduction

Reinforced concrete column elements experience a reduction in strength over time due to various loads such as compression, bending, etc. To enhance the compressive, moment, and shear capacities of existing columns, methods such as jacketing with fiber-reinforced materials or steel plates are commonly employed. However, these methods have disadvantages such as application difficulty, increased costs, and the unavailability of certain materials [1,2].

In Turkey, buildings constructed before 1997 face structural issues in their columns due to factors such as the non-mandatory use of ready-mix concrete, the use of plain (unribbed) reinforcement, and insufficient quality control during construction. As a result, reinforced concrete buildings may experience sudden collapses over time. This issue is not exclusive to Turkey but is prevalent in many other countries as well. Even in the absence of earthquakes, sudden collapses in buildings can occur due to inadequate cross-sectional dimensions and insufficient strength, leading to creep effects because the buildings are not constructed in accordance with national regulations. Retrofitting panels, which contain steel fibers, are essentially reinforced concrete elements and are more economical compared to other Retrofitting methods. Additionally, their production and application are extremely simple. Materials like CFRP can cause concrete disintegrate, especially when used in low-strength concrete, and if the jacketing covers the entire element, detecting this issue can be very challenging. Strengthening with steel profiles also has disadvantages, such as insufficient fire resistance. Therefore, using concrete panels for column retrofitting is expected to yield advantageous results. Based on the mechanical properties investigated in this study, column retrofitting studies will be undertaken [3,4].

In the literature, no similar studies on the retrofitting of reinforced concrete columns using steel-fibered concrete panels have been found. Buyukkaragoz (2020) previously conducted studies on strengthening masonry walls under shear using concrete panels, which yielded highly successful results. Experimental results on hollow brick walls and aerated concrete walls retrofitted with fiber-reinforced concrete panels indicated that the retrofits applied to the aerated concrete were more effective. Notably, the experiments revealed that the retrofitted test elements remained intact as a whole, even after failure [3,5,6].

As is well known, concrete serves as a quintessential example of a quasi-brittle material, posing a persistent challenge in the context of fracture failure within materials science and engineering, as discussed by Han et al. (2024) in their examination of the quasi-brittle nature of various engineering materials. Therefore, for decades, both three-point and four-point flexural strength tests have been implemented to represent the tensile strength of concrete through the modulus of rupture. Furthermore, by virtue of the quasi-brittle nature concrete, prior studies such as Osgouei et al. (2023) indicated that most of the tested beams were fabricated with initial notches to induce the first crack at the mid-span of the beam, and finite element models (FEM) were subsequently developed accordingly. Even concrete structures fabricated with advanced technologies to produce thin, resilient concrete, such as those studied by Eller et al. (2023), cannot be accurately represented by feasible finite element models due to the quasi-brittle nature of concrete and the thinness of the concrete body [6–8].

In this study, the concrete panels employed for retrofitting contain steel fibers at volume fractions of 0%, 1%, and 2%. Based on previous studies, the effective volume fraction of steel fibers ranges from 0% to 2%. Additionally, exceeding a volume fraction of 2% can lead to agglomeration. These panels were produced with a thickness of 10 mm, and the steel fibers used were Dramix ZP 305 fibers, manufactured in accordance with ASTM A820 [9] standards [10–12].

Given the lack of definitive recommendations from prior studies regarding finite element modeling of thin steel-fibered concrete, the current investigation aims to make a concerted effort towards addressing this gap. To achieve and elucidate this objective, a flowchart has been developed and is presented in Figure 1.

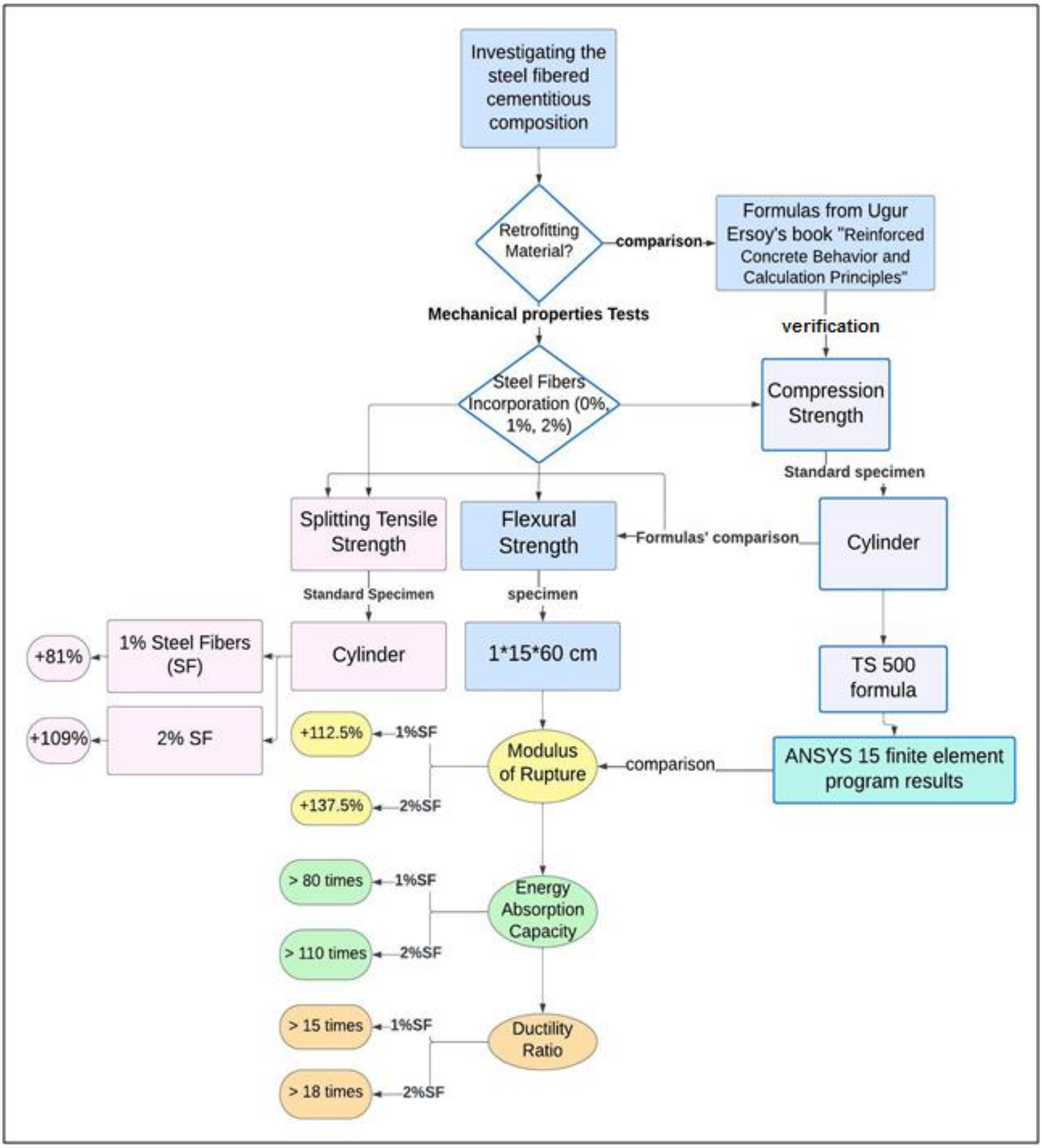

Fig. 1. Schematic Flowchart Outlining the Methodology and illustrating the Conceptual Framework of the Current Investigation.

Nomenclature

FEM finite element model
w/c wate-cement ratio

SF steel-fiber
Sp: specimen
P_P: peak load
P_u: ultimate load
Δ_P: peak displacement
Δ_u: ultimate displacement
Δ_y: the model's maximum y deflection
F_c: compressive strength of cylindrical specimens
F_{ct}: splitting tensile strength
F_{ctf}: splitting tensile formula
σt: bending strength capacity or Modulus of Rupture
σ_{tf}: formula of Modulus of rupture
σ_x: modeled Bending strength capacity
μ: ductility ratio
E_f: energy consumption
incr.: increment

2. Experimental program

2.1. Mixture

In the TS EN 206 standard [13], concrete is defined as a material that acquires the necessary properties through cement hydration, formed by a mixture of fine aggregate, coarse aggregate, cement, and water, with or without the addition of mineral and chemical admixtures. Due to the 10 mm thickness of the panels, coarse aggregate was not utilized. The materials used in the production of the panels are listed in Table 1 [14].

Table 1. Mixture Design of Cement Mortar.

Materials	Weight (kg/m^3)
Cement	955
Aggregate	992
Water	305
constituents' weight	2252
w/c	0.33
Superplasticizer	2.75%
Steel-fiber SF	0%, 1%, 2%

2.1.1. Cement

In this study, CEM I 32.5 R type cement, compliant with TS EN 197-1 [15] standards, was utilized [16].

2.1.2. Aggregate

Throughout the panel manufacturing process, only sand was employed, with a maximum particle size of 16 mm, ensuring compliance of the aggregate with TS EN 802 [17] and ASTM C1116 [18] standards.

2.1.3. Water

As stated in TS EN 1008 [19], if water is potable, it can also be used as mixing water. The mixing water used in concrete construction serves three purposes: curing, washing, and mixing. The water used is sourced from potable water flowing through the city water network. In accordance with the specifications outlined in ASTM C1116 [18], ensure that the pH value of the mixing water is 7 or above, and that it appears pure and colorless.

2.1.4. Superplasticizer

In this study, Sikament FFN was used as a superplasticizer admixture for concrete, which significantly reduces the mixing water content while enhancing both early and final strengths, or imparts high fluidity to the concrete with the same amount of water. This usage conforms to the specifications outlined in TS EN 934-2 [20] Tables 3.1 and 3.2. Due to significantly low w/c ratio, the relatively fine maximum particle size of the aggregate, and the inclusion of steel fibers in the current study, adding a superplasticizer is highly essential [21,22].

2.1.5. Steel-fiber

Steel fibers are steel materials utilized in the construction industry as an alternative to mesh reinforcement. They enhance properties such as the strength, toughness, and resistance to cracking and abrasion of concrete. Typically, these steel fibers are circular in cross-section, although rectangular cross-sections are also used. The lengths of these fibers range from 30 to 60 mm, with diameters between 0.5 and 1.0 mm, and their tensile strengths vary from 345 N/mm² to 2000 N/mm². Steel fibers with hooked ends provide higher adhesion compared to those with straight ends [23,24].

The volume fractions of steel fibers added to concrete can vary between 0.5% and 2.5%. Research indicates that adding more than 2% steel fibers can affect the formation of smooth surfaces and adhesion in 10 mm thick panels, with optimal benefits achieved at a ratio of 1-2% [25,26].

The properties of the steel fibers (Dramix ZP305) used in this study, produced in accordance with ASTM A820 [12], are detailed in Table 2. below. These Dramix ZP305 fibers have hooked ends to ensure better adhesion.

Table 2. Dramix ZP305 Features.

Physical and mechanical	properties
length (mm)	60
Diameter (mm)	0.9
Aspect ratio	65
Net weight gr/cm3	7.85
Tensile strength MPa	1250

2.2. Test setup and instrumentation

Determining the mechanical properties of the concrete mixtures used is of great importance for both analytical and numerical analysis. Therefore, this section evaluates the compressive strength, splitting tensile strength, and three-point bending strength tests in terms of experimental conditions, the standards employed, and the results obtained.

2.2.1. Compressive strength

The test method was conducted in accordance with ASTM C39M [27]. For determining the compressive strength of the panels, a total of nine samples were used for each designed compressive strength category, as shown in Figure 2. The cylindrical specimen had dimensions of 200 mm in height and 100 mm in diameter, as shown in Figure 2.a [27].

The compressive strengths of the panels, based on the volume fractions of steel fibers, are provided in Table 3. The test device features a motor-controlled hydraulic loading system with an adjustable speed, allowing the experiments to be performed at a fixed loading rate. For all test specimens, a loading rate of 3.1 kN/s was applied, as depicted in Figure 2.b [27].

Fig. 2. illustrates the compressive strength test of the concrete used in the panels: a) the failure modes of the elements depending on the steel fiber ratio, b) the display panel for test results on the test apparatus.

Table 3. Compressive Strength of the Panels.

volume fraction (vf)	0%	1%*	2%*
specimen 1	43.48	52.39	54.88
specimen 2	45.40	54.71	57.21
specimen 3	48.54	51.19	53.52
Average	45.81	52.76	55.21

* Mixtures containing steel fibers have not exhibited any significant cracks.

2.2.2. **Splitting tensile strength**

As is known, there are three distinct experimental methods for determining concrete tensile strength: the direct tension test, the bending test, and the split tension test. The tensile strength results obtained using these methods differ from one another. Therefore, when reporting the tensile strength of concrete, it is essential to specify which method was employed. In the split tension test, the tensile stress developed in cylindrical specimens is calculated using Eq.1.

$$f_t = \frac{2*P}{\pi*L*D} \tag{1}$$

Herein, P represents the compressive load applied to the cylinder, L denotes the length of the cylindrical specimen, and D is the diameter of the cylindrical specimen. [28–30]

This test method was conducted as described in the ASTM C 496/C 496M – 04 [25] standard. Nine cylindrical specimens measuring 200x100mm were utilized for this purpose. The experiment was carried out using a testing device with an axial load capacity of 1000 kN, located at the Structural Mechanics Laboratory of the Faculty of Technology, Civil Engineering Department, Gazi University. As shown in Figure 3.a, a compressive load was applied to the upper and lower bearing strips at a rate of 10 kN/s. As illustrated in Figures 3.b and 3.d, the cylinders reinforced with steel fibers exhibit no signs of disintegration. Conversely, as depicted in Figure 3.c, the cylinders lacking steel fibers have fractured into two distinct pieces [25].

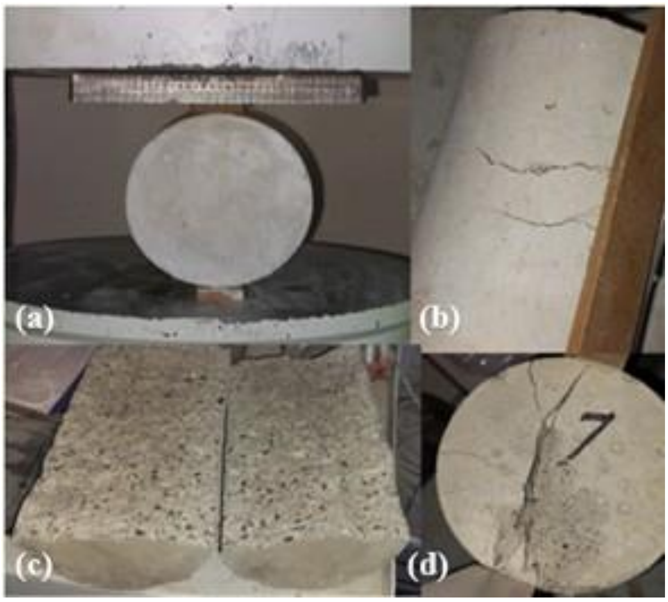

Fig. 3. Splitting Tensile Strength of Panels: a) cylinder splitting test, b) cylindrical test specimen without steel fibers, c) inability to split the cylindrical specimens containing 1% and 2% steel fibers under the splitting load, d) the cylindrical specimens containing 1% and 2% steel fibers remain intact without splitting under the load.

The experimental results are presented as averages in Table 4. Furthermore, the results obtained from the experiments have been compared to evaluate the Split Tension formula of ACI-318 [31], as shown in Tables 2 and 3 [28][32,33].

Table 4. Results of the Cylinder Splitting Test.

SF (%)	Sp.* 1	Sp.* 2	Sp.* 3	Average (MPa)
0	3.499	3.945	3.325	3.590
1	6.555	6.264	6.657	6.491
2	7.586	7.474	7.474	7.511

* Sp is the abbreviation for specimen.

2.2.3. Three point flexural strength

The bending test was conducted to determine design information about the material's strength and to identify the mechanical properties of the material against bending. One face of column elements subjected to horizontal loads (such as seismic loads) is exposed to bending. The fundamental principle of this test is to observe the performance of the plates used in the test under bending. Since the column equation is derived based on the ideal moment condition, it is desired that the shear stress in the column remains negligible compared to the normal stresses. [34,35] When a force is applied to the test specimen, if compressive stress occurs in part of the specimen's section and tensile stress occurs in the remaining part, the specimen is in a state of bending. In specimens under bending, compressive stresses develop in regions close to the upper surface, while tensile stresses develop in regions close to the lower surface. Terms used in the bending test include:

Bending moment (M), Bending stress (σ), Load (P), Distance between supports (L), Moment of inertia (I), Distance from the section's centroid to the outermost layer (c).

$$M = \frac{P*L}{4} \quad (2)$$

$$\sigma = \frac{M*c}{I} \quad (3)$$

For the successful execution of the bending test, certain steps must be followed. Initially, the diameters of the supports and the mandrel were determined to be suitable for the material to be used. Additionally, the span between the supports was adjusted in accordance with the relevant standard ASTM C 293 [36] and C 78 [34,37–39]. After the apparatus was set up, the specimen was placed on the supports and loading was initiated on the test element. The load was applied through the mandrel, subjecting the element to bending forces. At the start of the test, the load was applied along the cross-section at the center of the panel. During the loading process, load and displacement measurements were obtained using a computer program compatible with the test setup. Since the panels tested will be applied to sparsely spaced stirrup columns at a 1/3 scale, these panels were designed and manufactured in the dimensions of 10 x 100 mm and 10 x 150 mm, as shown in Figure 4.

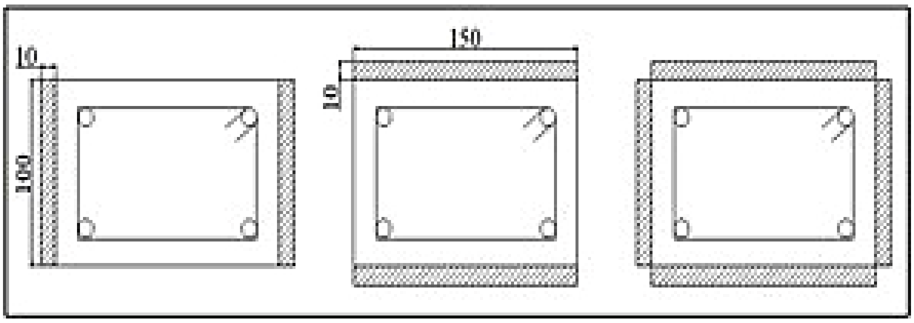

Fig. 4. Representation and Dimensions of Steel Fiber Panels on Columns.

The experiments were conducted using the three-point bending test apparatus located in the Construction Laboratory of the Civil Engineering Department at Ankara University, as shown in Figure 5. The test apparatus is equipped with a motor-controlled hydraulic loading system with adjustable speed, allowing the experiments to be performed at a constant loading rate. The experiments were carried out at a relatively slow loading rate of 1 kN/s to observe the response of the plates to loading after the initial crack.

During the experiments, an electronic displacement measurement device, referred to as the Three-Point Bending Test Apparatus, was used. This device measures displacements in various directions with an accuracy of 0.0001 mm and transfers these measurements to a computer via a data collector. For each test specimen, a load-displacement graph was plotted. Measurements for all test specimens were taken from the midpoint of load application. A total of nine panels were used for this test. Thus, due to the thinness of the panels and the necessary sensitivity to carry out the experiment, the average results of three panels for each mixture were used. The test procedure for a test specimen is shown in Figure 6. The distance between the two supports is L=540 mm, and the edge distance on both sides is 30 mm.

The load-displacement curves obtained from the test specimens are presented in Figure 7. The area under the load-displacement curves represents the amount of energy consumed, and the obtained values are provided in Table 2.5. The peak load (P_P) represents the maximum bending load which is experienced by each plate whereas the ultimate load denotes the point of failure, occurring when the loading decreases to reach 80% of the peak load.

Fig. 5. Three-Point Bending Test Apparatus Located in the Construction Laboratory of the Civil Engineering Department at Ankara University.

Fig. 6. Three-Point Bending Test.

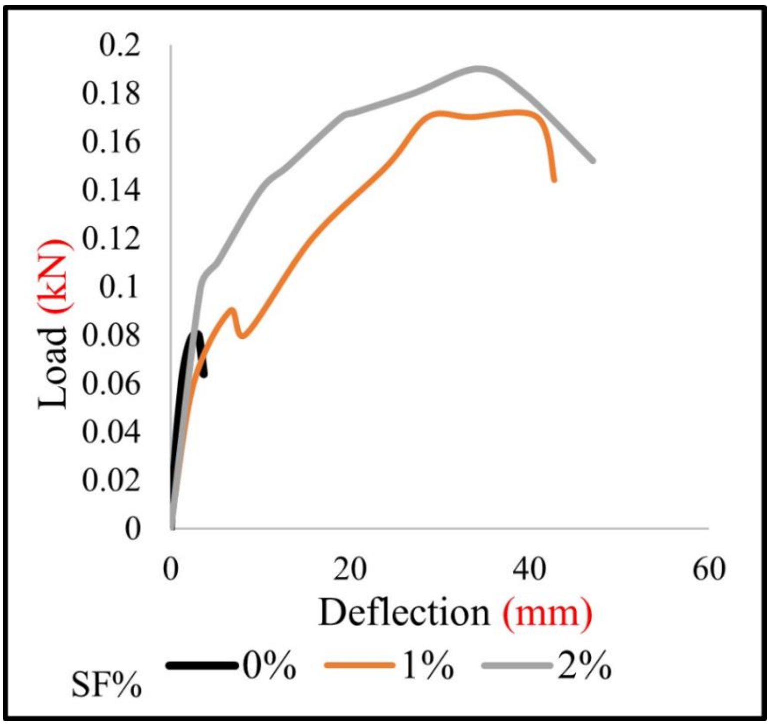

Fig. 7. Load-Displacement Curves of the Panels.

3. Results and analysis

In the current study, only the mechanical properties of the panels, specifically the results from compressive and tensile tests, are presented. The average results of the three experiments described in the Experimental Program section are compiled in Table 5. All formulas presented in this section are valid only for a mixture with a 0% volume fraction of steel fibers. The aforementioned formulas do not take into account the effects of steel fiber reinforcement or high-strength concrete. Nevertheless, the obtained results have been used for comparison purposes or to analyze the enhancements provided.

Table 5. Tests Results.

SF (%)	F_c (MPa)	Increment (%)	F_{ct} (MPa)	σ_t (MPa)
0	45.81	0	3.59	4.32
1	52.76	15.2	6.49	9.18
2	55.21	20.8	7.51	10.26

3.1. Splitting tensile strength test analysis

In order to effectively analyze and evaluate the increase provided by adding steel fibers to the proposed retrofitting panels in the mixture through splitting tensile tests, the increases have been calculated compared to the steel fiber-free mixture as shown in Table 6. Additionally, for comparative purposes, the modified formula of the Brazilian tensile method specified in ACI-318 [31] was utilized.

$$f_{ct} = 0.56\sqrt{f_c}\,(\text{MPa}) \quad (4)$$

fc: represents the compressive strength obtained from the experiments [28,33].

Table 6. Analysis of Splitting Tensile Strength Test.

SF (%)	F_{ct} (MPa)	increment (%)	F_{ctf} (MPa)
0	3.590	0	3.698
1	6.491	80.8	3.932
2	7.511	109.2	4.061

When the ratio of the experimental result of the steel fiber-free mixture to the result obtained from the analytical formula is examined, a ratio of 0.97 is obtained. This result indicates that the experimental and analytical formula results are very close.

3.2. Three point flexural strength test analysis

Similar to the Splitting Tensile Strength, the three-point bending beam experiment is also illustrated in Table 3.3. As referred to, the three-point modulus of rupture can be calculated in accordance with the formula:

$$\sigma_t = 0.70\sqrt{f_c}\,\text{Mpa} \quad (5)$$

Table 7. Analysis of the Three-Point Bending Beam Experiment.

SF (%)	σ_t (MPa)	Increment (%)	σ_{tf} (MPa*)
0	4.32	0	4.62
1	9.18	112.5	4.92
2	10.26	137.5	5.08

*Ugur Ersoy, "Reinforced Concrete Behavior and Calculation Principles", Three Point Flexural Strength Test [28].

The area under the load-displacement curves in Fig. 7. represents the energy consumed up to the collapse point of the panels (E_f), as provided in Table 3.4. Ductility is the capacity to undergo deformation without significant loss in strength. Consequently, the variation in ductility ratios among the test specimens indicates the behavior exhibited after the onset of plasticization. The ductility ratio (μ) is derived from the load-displacement graph shown in Fig. 7. by dividing the yield displacement (initial crack or 0.75Pp) by the ultimate displacement.

(collapse crack or 0.8Pp). The ductility ratio (μ) has been calculated using Eq.6 and is presented in Table 8:

$$\mu = \frac{\delta u}{\delta y} \quad (6)$$

Where (μ) represents the ductility ratio, (δy) is the displacement at the initial crack or 0.75Pp, and (δu) is the displacement at the collapse crack or 0.8Pp. [40,41]

Table 8. Ductility ratio and Energy consumption values.

SF (%)	μ	Incr. (%)	E_f (N.mm)	Incr. (%)
0	1.11	0	70	0
1	17.81	1504	5100	7185
2	21.41	1828	7010	9914

4. Three point flexural strength fe modelling

In this section, the three-point bending beam experiment has been modeled using the ANSYS 15 finite element principle. The formulas and experimental results mentioned in Chapter 3 of the study have been tested. However, the closest result to the tensile test in bending, which was given by the direct tensile formula TS500-2000 [42]:

$$f_{ct} = 0.35\sqrt{f_c} \tag{7}$$

In addition, it is presented in Table 9. Since this formula does not consider the effect of steel fibers, it was assumed that the steel fibers are distributed horizontally at a 45-degree angle in all directions in the concrete modeling using the Solid65 element type in the ANSYS program. The maximum load obtained from each test specimen was applied to the test model by taking advantage of non-linear analysis. Additionally, the same loading and support conditions were applied. The compressive stress capacity is provided in Table 10. As the error rate did not exceed 10%, the model can be considered acceptable. To assign the modeled bending strength capacity, the stress in the X-direction was utilized, as it corresponds to the resultant stress. [43–45].

Table 9. The values of the TS500-2000 formula in the modeling.

SF %	Direct tensile formula (MPa)
0	2.312
1	2.457
2	2.537

Table 10. Flexural strength capacity and the maximum stress resistance obtained from the modeling.

SF (%)	σt (MPa)	σ_x (MPa)	Error %	Δ_y (mm)
0	4.32	-4.25	1.6	2.57
1	9.18	-8.90	3.1	4.51
2	10.26	-9.9	3.5	5.42

- The model of the three-point bending beam with steel fibers at a volume fraction of 0 percent; as illustrated in Figure 8, subsequent to the application of support and loading conditions, the state of the beam post-deformation and the stress values.
- The model of the three-point bending beam with steel fibers at a volume fraction of 1 percent; as illustrated in Figure 9, subsequent to the application of support and loading conditions, the state of the beam post-deformation and the stress values.
- The model of the three-point bending beam with steel fibers at a volume fraction of 2 percent; as depicted in Fig. 10, following the application of support and loading conditions, the post-deformation state of the beam and the stress values.

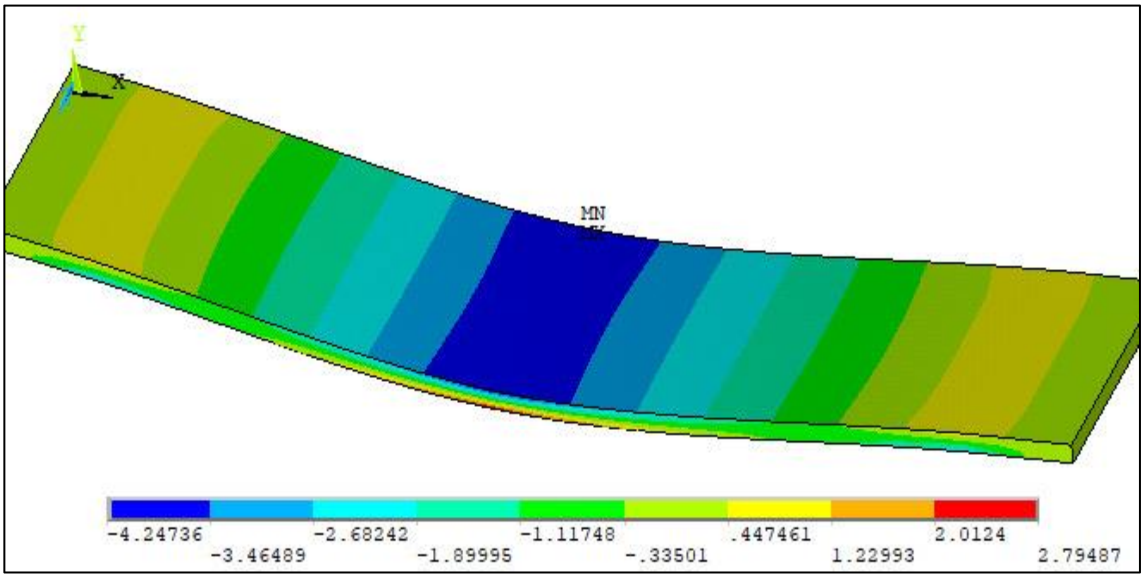

Fig. 8. The model of the three-point bending beam with a 0% volume fraction of steel fibers.

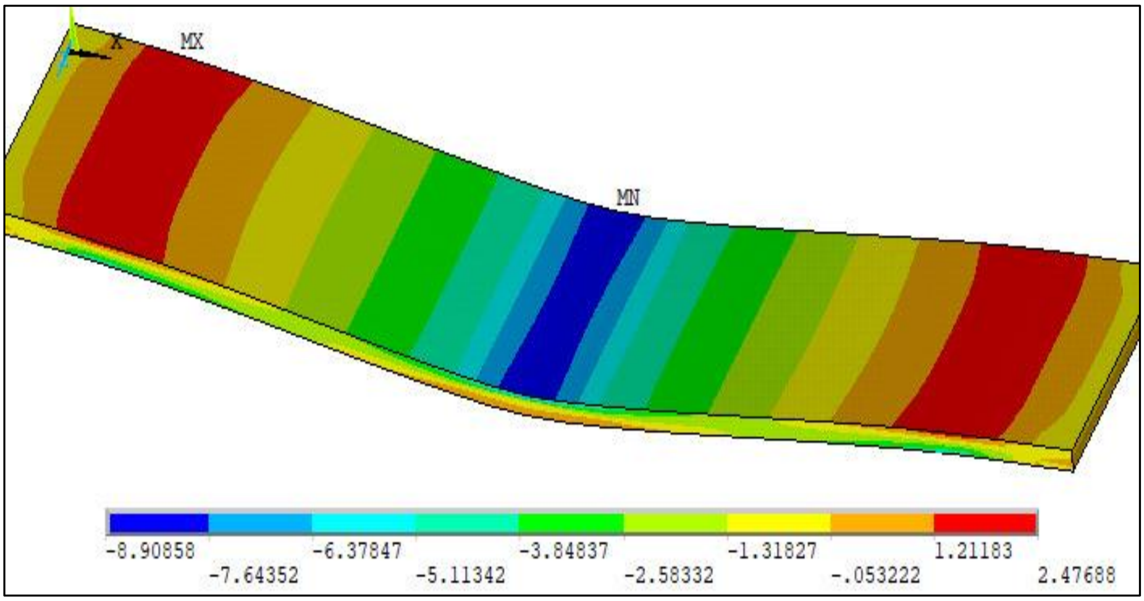

Fig. 9. The model of the three-point bending beam with a 1% volume fraction of steel fibers.

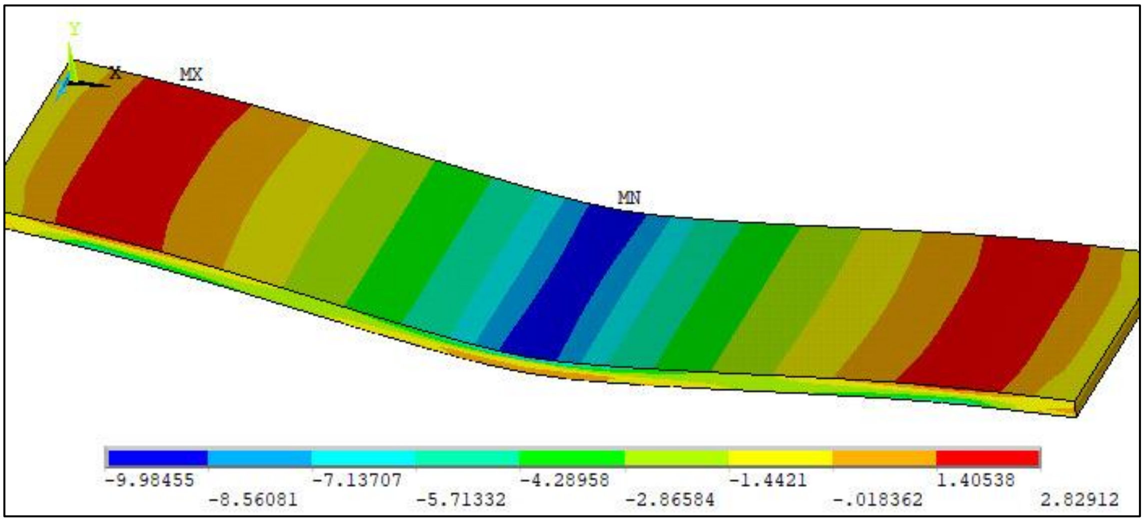

Fig. 10. The model of the three-point bending beam with a 2% volume fraction of steel fibers.

5. Conclusion

As mentioned in the literature review section of the introduction, there is currently no viable model for thin concrete, nor is there any material that can accurately represent steel-fibered concrete or ductile concrete in ANSYS or any other finite element method (FEM) program. Therefore, both linear and non-linear analyses were utilized, incorporating numerous presumptive results and formulas, in an effort to develop the most feasible and realistic model possible. In this section, experimental results have been compared with analytical and numerical results.

- It has been observed that the inclusion of steel fibers offers a limited increase in compressive strength, yet markedly enhances the tensile strength.
- As demonstrated in the splitting tensile strength section, cylinders without steel fibers were bisected, while those containing 1% and 2% volume fractions of steel fibers experienced only compression. Similarly, panels reinforced with steel fibers, as shown in the three-point flexural strength section, remained intact. The inclusion of steel fibers significantly contributed to preserving the structural integrity of the elements, thereby enhancing the overall safety and longevity of retrofitted structures, along with facilitating the repair and replacement of these retrofitting plates.
- The incorporation of steel fibers into concrete at volume fractions of 1% and 2%, respectively, has resulted in an increase in split tensile strength by 80.8% and 109.2% in this study.
- The addition of steel fibers to concrete at volume fractions of 1% and 2% has been observed to increase the tensile strength in bending by 112.5% and 137.5%, respectively, in this study.
- Due to the 10 mm thickness of the panels and the semi-rigid behavior of the concrete, increasing the steel fiber content to 1% and 2% augmented the energy absorption capacity by 7995% and 11027%, respectively, and the ductility ratio by 1504% and 1828%, respectively.
- As seen in load-deflection curves, steel fiber-reinforced panels consume significantly more energy compared to non-steel fiber panels until they reach their capacity and fail. Due to this contribution, it is believed that these panels can provide a certain level of ductility to columns with low ductility ratios.
- This study aligns with the findings of previous research. Yavuz Bayraktar et al. (2023) reported significant increases in compressive strength, splitting tensile strength, and flexural strength when using steel fibers with less than 1% volume fraction and a length of 30 mm. The compressive strength results obtained in this study are consistent with those reported by Yavuz Bayraktar et al. (2023). While their study achieved higher compressive strength, the splitting tensile and flexural strengths observed were either equivalent to or lower than those in the present study [25].

Several key factors may contribute to these differences:

1. Fiber Length: The length of steel fibers plays a critical role, as shorter fibers tend to enhance compressive strength while potentially reducing tensile strength [46].
2. Incorporation of Additives: The addition of materials such as limestone and recycled fine aggregate can significantly influence the overall performance characteristics of the composite material.
3. Volume Ratio Changes: Variations in the volume fractions of steel fibers used in the two studies may also account for the observed differences in mechanical properties.

In conclusion, the results of the current study are compatible with those of Yavuz Bayraktar et al. (2023), highlighting the importance of fiber length, additive inclusion, and volume fraction in governing the mechanical behavior of steel fiber-reinforced concrete composites [25,46].

The results obtained from the modeling study were also compatible with the values obtained from the experimental results.

- The stress results from the modeling were consistent with the experimental data, showing a maximum error rate of 3.5%. However, due to the Solid 65 element's compatibility with thicker reinforced concrete, full alignment could not be achieved between the displacement values obtained from the modeling of thin steel-fibered concrete plates and the experimental results.
- Following the completion of the tests and modeling, significant enhancements attributed to the inclusion of steel fibers were observed. Consequently, steel-fibered concrete panels were utilized to retrofit 30 columns subjected to axial loading, employing epoxy as the adhesive material. This retrofitting approach resulted in substantial improvements, with the loading capacity and energy absorption capacity increasing by 71% and 428%, respectively. Furthermore, the strengthening method demonstrated advantages in terms of cost-effectiveness, ease of application, and rapid implementation.
- The fabricated plates can be employed to rehabilitate or retrofit a wide range of construction components and structural types. Moreover, considering the cost-effectiveness of the retrofitting or rehabilitation process, along with the ease of application and molding, these plates may facilitate the incorporation of concrete additives to produce higher-quality concrete, potentially enabling the use or combination of different types of fibers.

Funding

No funding was received for this research.

Conflicts of interest

All authors declare that they have no conflicts of interest.

Authors contribution statement

Omer M. M. Mahdi: Data curation; Formal analysis; Investigation; Methodology; Project administration; Resources; Software; Validation; Visualization; Roles/Writing – original draft; Writing – review & editing.

Alper Buyukkaragoz: Conceptualization; Data curation; Formal analysis; Investigation; Methodology; Project administration; Resources; Software; Supervision; Validation; Visualization; Roles/Writing – original draft; Writing – review & editing.

Ahmet S. Unal: Data curation; Formal analysis; Investigation; Methodology; Resources; Software; Validation; Visualization; Roles/Writing – original draft.

References

[1] Mercimek Ö, Ghoroubi R, Anil Ö, Çakmak C, Özdemir A, Kopraman Y. Strength, ductility, and energy dissipation capacity of RC column strengthened with CFRP strip under axial load.

Mech Based Des Struct Mach 2023;51:961–79. doi:10.1080/15397734.2020.1860772.

[2] Yooprasertchai E, Juntanalikit P, Jirawattanasomkul T, Srivaranun S, Pimanmas A. Cyclic performance of non-ductile reinforced concrete columns retrofitted by partial steel plate jacketing: Experiment and numerical analysis. Struct Concr 2024. doi:10.1002/suco.202300326.

[3] Buyukkaragoz A. Shear behavior of aerated concrete and hollow brick walls strengthened with steel fiber-reinforced concrete panels. Mech Adv Mater Struct 2020;27:1531–9. doi:10.1080/15376494.2018.1519617.

[4] Bedirhanoglu I, Ilki A, Triantafillou TC. Seismic Behavior of Repaired and Externally FRP-Jacketed Short Columns Built with Extremely Low-Strength Concrete. J Compos Constr 2022;26. doi:10.1061/(ASCE)CC.1943-5614.0001179.

[5] Choudhary S, Jain A, Bhavsar H, Chaudhary S, Choudhary R. Analysis of steel fiber reinforced concrete wall panels under compression, flexural and impact loading. Mater Today Proc 2021;38:2471–5. doi:10.1016/j.matpr.2020.07.509.

[6] Osgouei YB, Tafreshi ST, Pourbaba M. Flexural Properties of UHPFRC Beams with an Initial Notch. J Rehabil Civ Eng 2023;11:141–77. doi:10.22075/JRCE.2022.25513.1576.

[7] Han X, Li P, Liu J. Application of a Closed-Form Model in Analyzing the Fracture of Quasi-Brittle Materials. Materials (Basel) 2024;17:282. doi:10.3390/ma17020282.

[8] Eller B, Movahedi Rad M, Fekete I, Szalai S, Harrach D, Baranyai G, et al. Examination of Concrete Canvas under Quasi-Realistic Loading by Computed Tomography. Infrastructures 2023;8:23. doi:10.3390/infrastructures8020023.

[9] Specification for Steel Fibers for Fiber-Reinforced Concrete 1996. doi:10.1520/A0820-96.

[10] Zhang P, Wang C, Gao Z, Wang F. A review on fracture properties of steel fiber reinforced concrete. J Build Eng 2023;67:105975. doi:10.1016/j.jobe.2023.105975.

[11] Ge L, Zhang Y, Feng Z, Li H. Study on the mechanical and microscopic properties of steel fiber reinforced reactive powder concrete under different curing methods. J Build Eng 2023;76:107436. doi:10.1016/j.jobe.2023.107436.

[12] Wang Z, Li H, Zhang X, Chang Y, Wang Y, Wu L, et al. The Effects of Steel Fiber Types and Volume Fraction on the Physical and Mechanical Properties of Concrete. Coatings 2023;13:978. doi:10.3390/coatings13060978.

[13] Asim Y, Tomris E. TS EN 206-1, Concrete- Part 1: Specification, performance, production and conformity. Ankara: 2002.

[14] Pourghashti HH, Madandoust R, Ranjbar MM. Studying Tensile Strength of the Recycled Coarse Aggregate Concrete Using Double-Punch Test. J Rehabil Civ Eng 2022;10:100–20. doi:10.22075/JRCE.2021.20395.1413.

[15] TS EN 197-1, Cement - Part 1: Composition, specifications and conformity criteria for common cements. Eur Stand n.d.;603.

[16] Müller C. How standards support sustainability of cement and concrete in Europe. Cem Concr Res 2023;173:107288. doi:10.1016/j.cemconres.2023.107288.

[17] TSE. TS 802 Beton karışımı hesap esasları. TS 802 Bet Karışımı Hesap Esasları 2016.

[18] ASTM. ASTM C1116/C1116M-10a, Standard Specification for Fiber-Reinforced Concrete. ASTM 2023.

[19] Turkish Standard. TS EN 1008. TS 2003.

[20] Turkish Standard. TS EN 934-2. TS 2010.

[21] Cavusoglu I, Yilmaz E, Yilmaz AO. Additivity effect on properties of cemented coal fly ash backfill containing water-reducing admixtures. Constr Build Mater 2021;267:121021. doi:10.1016/j.conbuildmat.2020.121021.

[22] Cemalgil S, Onat O, Aruntaş HY. An Estimation Proposal for Engineering Properties of Modified Concrete by using Standalone and Hybrid GRELM. Iran J Sci Technol Trans Civ Eng 2023;47:1357–77. doi:10.1007/s40996-022-01005-6.

[23] Lanwer J-P, Empelmann M. Performance-Based Fibre Design for Ultra-High Performance Concrete (UHPC). Appl Sci 2022;12:8559. doi:10.3390/app12178559.

[24] Ni W, Cui X, Yuan J, Sun W, Cui C, Wu Y, et al. The influence of fiber, aggregate and cementitious materials on the mechanical properties of ultra-high content steel fiber reinforced reactive powder concrete. Constr Build Mater 2024;431:136530. doi:10.1016/j.conbuildmat.2024.136530.

[25] Yavuz Bayraktar O, Kaplan G, Shi J, Benli A, Bodur B, Turkoglu M. The effect of steel fiber aspect-ratio and content on the fresh, flexural, and mechanical performance of concrete made with recycled fine aggregate. Constr Build Mater 2023;368:130497. doi:10.1016/j.conbuildmat.2023.130497.

[26] Biswas RK, Bin Ahmed F, Haque ME, Provasha AA, Hasan Z, Hayat F, et al. Effects of Steel Fiber Percentage and Aspect Ratios on Fresh and Harden Properties of Ultra-High Performance Fiber Reinforced Concrete. Appl Mech 2021;2:501–15. doi:10.3390/applmech2030028.

[27] ASTM International. Standard Test Method for Compressive Strength of Cylindrical Concrete Specimens 1 - ASTM C39/C39M - Standard. Annu B ASTM Stand 2021;04.02:1–7.

[28] Ersoy U., Canbey E. OG. Betonarme Cilt 1 Davranıs ve Hesap İlkeleri (Turkish Language). Turkey: 2020.

[29] H BS. Numune Şekli ve Boyutunun Lif ve Lif İçermeyen Beton Karışımlarının Dayanımına Etkisi (Turkish). Uludag university, 2018.

[30] ASTM. C 496/C 496M, Standard Test Method for Splitting Tensile Strength of Cylindrical Concrete Specimens. ASTM 2017. doi:DOI: 10.1520/C0496-96.

[31] ACI. ACI 318-19: Requisitos de reglamento para concreto estructural y comentario de requisitos de reglamento. Am Concr Inst 2019:1–688.

[32] Yu W, Jin L, Du X. Experimental investigation on splitting-tension failures of basalt fiber-reinforced lightweight aggregate concrete: Effects of strain rate and structure size. J Build Eng 2023;68:105853. doi:10.1016/j.jobe.2023.105853.

[33] Wong ILK. Effect compressive strength and split tensile strength of concrete using aggregate from Tana Toraja district with fly ash substitution. IOP Conf Ser Earth Environ Sci 2021;921:012066. doi:10.1088/1755-1315/921/1/012066.

[34] Ren H, Li T, Ning J, Song S. Bending damage and fractal characteristics of steel fiber-reinforced concrete under three-point bending test. Constr Build Mater 2023;409:134053. doi:10.1016/j.conbuildmat.2023.134053.

[35] Saatci S, Cetin FS, Aloui S, Naseri J. Effects of steel fiber type and ratio on the one-way bending behavior of hybrid fiber reinforced concrete thin panels. Constr Build Mater 2024;411:134190. doi:10.1016/j.conbuildmat.2023.134190.

[36] Test Method for Flexural Strength of Concrete (Using Simple Beam With Center-Point Loading) 2008. doi:10.1520/C0293-08.

[37] Test CC, Drilled T, Concrete C. Standard Test Method for Flexural Strength of Concrete (

Using Simple Beam with Third-Point Loading) 1. Hand 2010;C78-02:1–4.

[38] Li Y-F, Tsai P-J, Syu J-Y, Lok M-H, Chen H-S. Mechanical Properties of 3D-Printed Carbon Fiber-Reinforced Cement Mortar. Fibers 2023;11:109. doi:10.3390/fib11120109.

[39] Al-Rifaie WN, Ahmed WK, Mahdi OM. Green building using nano materials for high performance cement mortar composite. 2018 5th Int. Conf. Renew. Energy Gener. Appl., IEEE; 2018, p. 203–6. doi:10.1109/ICREGA.2018.8337578.

[40] Park.R. Structural Assemblages From Laboratory Testing. NZSEE – New Zeal Soc Earthq Eng 1989;22:155–66.

[41] Wu X, Kang THK, Mpalla IB, Kim CS. Axial Load Testing of Hybrid Concrete Columns Consisting of UHPFRC Tube and Normal-Strength Concrete Core. Int J Concr Struct Mater 2018;12. doi:10.1186/s40069-018-0275-2.

[42] TS500. Betonarme Yapıların Tasarım ve Yapım Kuralları. Turk Stand Enst 2000:1–75.

[43] Afanador García N, Guerrero Gómez G, Nolasco Serna C. Reinforced concrete beams subjected to three-point bending using finite element method. J Phys Conf Ser 2021;1938:012008. doi:10.1088/1742-6596/1938/1/012008.

[44] Pokorska I, Poński M, Kubissa W, Libura T, Brodecki A, Kowalewski Z. Computational Fracture Evolution Analysis of Steel-Fiber-Reinforced Concrete Using Concrete Continuous Damage and Fiber Progressive Models. Materials (Basel) 2023;16:5635. doi:10.3390/ma16165635.

[45] Xiang C, Shao W, Fang H, Liu Y. Failure predictions for steel-UHPC-steel sandwich beams under three-point bending. Ocean Eng 2023;288:116042. doi:10.1016/j.oceaneng.2023.116042.

[46] Han J, Zhao M, Chen J, Lan X. Effects of steel fiber length and coarse aggregate maximum size on mechanical properties of steel fiber reinforced concrete. Constr Build Mater 2019;209:577–91. doi:10.1016/j.conbuildmat.2019.03.086.